Available online at www.sciencedirect.com
SCIENCE DIRECT®
Biosensors and Bioelectronics 18 (2003) 1501–1508
BIOSENSORS & BIOELECTRONICS
www.elsevier.com/locate/bios

Electrochemical behavior and detection of hepatitis B virus DNA PCR production at gold electrode

Y.K. Ye [a], J.H. Zhao [b], F. Yan [b], Y.L. Zhu [a], H.X. Ju [a,*]

[a] Department of Chemistry, Institute of Analytical Science, State Key Laboratory of Coordination Chemistry, Nanjing University, Nanjing 210093, China
[b] Jiangsu Institute of Cancer Prevention and Cure, Nanjing 210009, China

Received 24 June 2002; received in revised form 29 January 2003; accepted 8 March 2003

Abstract

Sequence-known short-stranded hepatitis B virus (HBV) DNA fragment (181 bps) was obtained by PCR method. The strategy for its electrochemical detection was designed by covalently immobilizing single-stranded HBV DNA on gold electrode surface via carboxylate ester as a linkage between 3′-hydroxy end of DNA and carboxyl group of thioglycolic acid (TGA) self-assembled monolayer. The hybridization reaction on surface was evidenced by electrochemical methods using ferrocenium hexafluorophosphate ($FcPF_6$) as an electroactive indicator. The interactions of Fc^+ with single-stranded (ss) and double-stranded (ds) HBV DNA immobilized on TGA monolayer were studied. The difference between the responses of Fc^+ at ss- and ds-DNA/Au electrodes suggested that this hybridization biosensor could be conveniently used to monitor DNA hybridization with a high sensitivity. AC impedance and XPS techniques have been employed to characterize the immobilization of ss-DNA on the gold surface.

Keywords: Hepatitis B virus; PCR; Self-assembled monolayer; Biosensors; Ferrocenium hexafluorophosphate

1. Introduction

The detections of specific nucleic acid sequences of human, viruses and bacteria are becoming increasingly important in the diagnoses of diseases. Recently, some reports have exhibited that piezoelectric immunosensors (He and Zhang, 2002), chemiluminescent biosensors (Jiang et al., 2000), microfabricated disposable DNA sensors (Hashimoto et al., 1998), DNA optical sensors (Chen et al., 1998) and electrochemical biosensors (Meric et al., 2002; Wang et al., 1997; Marrazza et al., 2000) are suited for this purpose. Electrochemical DNA biosensors for recognition of DNA hybridization have been attracting increased attention (Wang, 1999; Erdem et al., 2000) because of their advantages such as low cost, simple design, small dimensions and low power requirements (Paleček and Fojta, 2001).

Persistent infection with hepatitis B virus (HBV) is a major health problem worldwide and may lead to chronic hepatitis, cirrhosis and primary liver cancer (Beasley, 1988). The detection of HBV DNA in the serum of patient is becoming an important tool in the diagnosis of HBV infection. The existence of HBV can be detected with a radioisotope tracer (RT) (Mendy et al., 1999; Ngui et al., 1999), which accounts for the emergence of the many natural mutants with point substitutions. Many non-radioactive methods such as the enhanced chemiluminescence (ECL) (Mendy et al., 1999) have also been used for detection of HBV. The development of genetic diagnosis makes it possible to detect and identify simultaneously viral molecules. The method is specific, sensitive, and rapid for the diagnosis of viral infection and the prediction of the chemotherapy (Yoshiko, 1999). Some commercial HBV monitors, such as Amplicor HBV Monitor (Roche Diagnostics Systems) (Gilbert et al., 2002; Poljak et al., 2001; Weber et al., 2001; Buffello-Le Guillou et al., 2000), Digene Hybride Capture System HBV Assay (Digene Corporation) (Gilbert et al., 2002; Buffello-Le Guillou et al., 2000; Pawlotsky et al., 1997), QUANTIPLEX HBV DNA Assay (Chiron Diagnostics Ltd.) (Gilbert et al.,

* Corresponding author. Tel./fax: +86-25-359-3593.
E-mail address: hxju@nju.edu.cn (H.X. Ju).

0956-5663/03/$ - see front matter
doi:10.1016/S0956-5663(03)00121-0

2002; Pawlotsky et al., 1997), TaqMan fluorogenic detection system (Mercier et al., 1999; Pas et al., 2000; Loeb et al., 2000), and AxSYM HBe 2.0 quantitative and liquid hybridization (Abbott Lab.) (Heijtink et al., 2001), have been used in clinical study. Enzyme immunoassay (Buffello-Le Guillou et al., 2000; Kimura et al., 2002), branched DNA signal amplification assay (Hwang et al., 1999; Lai et al., 1999) and nucleic amplification testing/technology (NAT) (Yates et al., 2001; Sato et al., 2001) have been used to detect quantitatively HBV DNA. Of the different types available to detect serum HBV DNA, the most sensitive method is to use target amplification techniques, such as the PCR (Gilbert et al., 2002; Poljak et al., 2001; Weber et al., 2001; Buffello-Le Guillou et al., 2000; Mercier et al., 1999; Pas et al., 2000; Loeb et al., 2000; Krajden, 1999; Poljak et al., 2001; Chen et al., 2001; Weber et al., 2001; Chemin et al., 2001; Mei et al., 2000; Shintani et al., 2000), which has been used as a routine method to amplify the HBV DNA target. Some commercial assays mentioned above such as Amplicor HBV Monitor and TaqMan fluorogenic diction system are based on PCR technique.

Here PCR method is used to amplify the HBV DNA fragments, and then the ss-DNA molecules are immobilized onto a TGA self-assembled monolayer on gold electrode surface. With a hybridization procedure, the complementary HBV DNA (cDNA) molecules bind with the immobilized ss-DNA to form ds-DNA on the electrode surface. The hybridization event is monitored with ferrocenium as an electrochemical hybridization indicator. This work uses PCR method to amplify the HBV DNA fragments and proposes a method to detect about 10^4 copies (about 1.7×10^{-20} mol or 0.7 fg) of original genomic HBV DNA. The sensitivity is higher than that of 0.2 mg l^{-1} (about 4×10^{-8} mol l^{-1}) 21-base target oligonucleotides based on an electrochemical method (Marrazza et al., 1999) and that of 50 nM of labeled probe based on an optical method (Rogers et al., 2001). It is even higher than that of 1–100 fg HIV-1 by combining surface plasmon resonance with PCR (Bianchi et al., 1997). Several electrochemical and spectra methods are used to study the ss-DNA immobilization on gold surface and the interaction between immobilized ss- or ds-DNA and Fc^+.

2. Experimental

2.1. Materials and reagents

Calf thymus DNA, 1-ethyl-3-(3-dimethyl-aminopropyl)carbodiimide (EDC) and Tris–(hydroxymethyl)aminomethane (Tris) were obtained from Sigma (USA) and used as received. Yeast DNA was from Changyang Chemical Factory (Shanghai, China), sodium dodecylsulfate (SDS) was purchased from Guangyao Chemical Reagent Co. (Jiangsu, China). All other reagents were of analytical reagent grade. All solutions were made up with twice-quartz-distilled water. Native ds-DNA was dissolved in 0.01 mol l^{-1} Tris–EDTA (TE) buffer (pH 8.0) prior to use. ss-DNA was produced by heating a native ds-DNA solution in a 100 °C water bath for about 5 min and then rapidly cooling in an ice bath.

2.2. Polymerase chain reaction

The first round of PCR amplification was performed on a standard Perkin–Elmer 9600 cycles (Perkin–Elmer, Warrington) using oligonucleotide primers 5′-CAT CAT CCT GGG CTT TC-3′ and 5′-AAA AAG GGA CTC AAG ATG TTG TA-3′ in 0.2 ml thin walled polypropylene tubes. The amplification mixture, in a final volume of 100 μl, contains 10.0 μl PCR buffer, 6.0 μl 25 mmol l^{-1} $MgCl_2$, 6.0 μl 20 mmol l^{-1} dNTPs, 3.0 μl of each primer, and 10.0 μl clinical control HBV DNA template with 1×10^7 copies that was known from the label. Before amplification cycles, the amplification mixture was predenatured at 100 °C for 5 min, then was added with 25 units Taq polymerase. The thermal program comprised an initial denaturation at 94 °C for 90 s followed by 40 amplification cycles. Each cycle included two steps: hold at 94 °C for 25 s, and at 60 °C for 60 s. After 40 amplification cycles, an extension step was performed at 70 °C for 10 min. Finally the mixture was conserved at 4 °C before use. Maximum ramp rates were used throughout. The fragments were separated with agarose gel electrophoresis to obtain 100 μl PCR product. The amplification product without further purification gave an A_{260}/A_{280} ratio of 1.82, thus the DNA was pure enough.

2.3. Immobilization of ss-DNA on TGA self-assembled monolayer

Gold electrodes (3 mm diameter) were firstly abraded successively with finer grades of SiC paper; then polished to a mirror-like surface with 0.05 μm alumina slurry on micro-cloth pads (Buehler) and ultrasonicated in turn with acetone and water for 3 min, respectively. The electrode was modified immediately by immersing it in 0.1 mmol l^{-1} TGA solution for 6 h to form TGA self-assembled monolayer on gold surface. Then the modified electrode was dipped in 0.1 ml HBV ss-DNA TE solution containing 0.1 μl PCR production and 0.04 mg EDAC for 1 h, which resulted in the covalent immobilization of ss-DNA on the modified gold electrode (Scheme 1) via carboxylate ester linkage between 3′-hydroxy end of DNA and carboxyl group of TGA (Zhao et al., 1999), named HBV ss-DNA/Au electrode. After the electrode was washed with 0.1% (m/m) SDS phosphate buffer (pH 7.0) and water, respectively. It

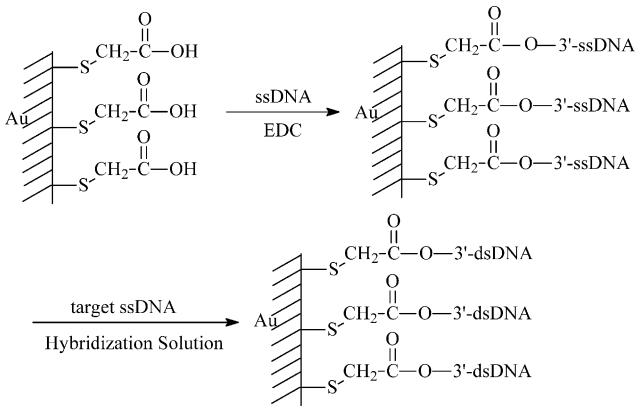

Scheme 1. Immobilization of ss-DNA on TGA monolayer modified Au electrode and hybridization of complementary target ss-DNA.

was stored in a 0.01 mol l^{-1} TE buffer (pH 8.0) prior to use.

2.4. Hybridization

Before hybridization, 0.1 ml buffer of 0.3 mol l^{-1} NaCl+0.03 mol l^{-1} sodium citrate containing 0.1 μl DNA PCR product (about 1×10^4 copies of original genomic HBV DNA) was reheated in a 100 °C water bath for about 5 min, then cooled slowly to about 55 °C. The HBV ss-DNA/Au electrode was immersed into the solution. The solution was then incubated in a water bath at 42 °C for 1 h to form ds-DNA at the electrode surface (Scheme 1), named HBV ds-DNA/Au electrode. As control, other DNA samples (denatured calf-thymus DNA and denatured yeast DNA) with a concentration of 0.1 mmol l^{-1} in the hybridization buffer were treated in the same way. After hybridization, the ds-DNA/Au electrode was washed with 0.1% (m/m) SDS phosphate buffer (pH 7.0) and water, respectively.

2.5. Apparatus and measurements

Electrochemical experiments were carried out at room temperature with a three-electrode system comprising a platinum wire as counter electrode and a saturated calomel electrode (SCE) as reference and a bare gold or DNA modified gold electrode as the working electrode. The electrodes were connected to a BAS-100B electrochemical analyzer with a PA-1 preamplifier (Bioanalytical System Inc., USA). The AC impedance experiments were carried out with CHI 660 Electrochemical Workstation (CH Instruments Inc., USA). All potentials were reported against the reference electrode without regard for the liquid junction. XPS spectra were performed on a VG ESCA-LAB MKII spectrometer (VG Co., UK) using a Mg radiation.

3. Results and discussion

3.1. Cyclic voltammetric (CV) experiments

Fig. 1 shows the cyclic voltammograms of 8.0×10^{-4} mol l^{-1} $FcPF_6$ at TGA/Au (a), ss-DNA/Au (b) and ds-DNA/Au (c) electrodes at 100 mV s^{-1}. A pair of redox peaks is observed at +332 and +90 mV at the TGA/Au electrode (Fig. 1a), which is attributed to the redox of Fc^+, respectively. At the ss-DNA/Au electrode, the redox peak currents of Fc^+ increase obviously (Fig. 1b), and the peak potentials become +388 and +80 mV, respectively. From the reduction peak area of Fc^+, the surface absorbance of Fc^+ on the ss-DNA/Au electrode is obtained to be 2.64×10^{-9} mol cm^{-2}. After hybridization of the immobilized ss-DNA with cDNA, the peak currents of Fc^+ are lower than those before hybridization, and the redox peaks occur at +372 and +82 mV, respectively (Fig. 1c). The anodic and cathodic peak currents decrease by 70.8 and 21.7%, respectively. The lower peak currents of Fc^+ at the ds-DNA/Au electrode are indicative of a weaker electrostatic interaction between Fc^+ and the immobilized ds-DNA helix, than that at the ss-DNA/Au electrode (Zhao et al., 1997). In comparison with that at the TGA/Au electrode, the cathodic peak potentials of Fc^+ at both ds-DNA/Au and the ss-DNA/Au electrodes shift towards the negative direction. Such behavior is characteristic of electrostatic interaction of Fc^+ with DNA (Carter et al., 1989; Rodriguez and Bard, 1990), which makes the reduction of Fc^+ at the surface with negative charge more difficult.

With increasing scan rate from 100 to 700 mV s^{-1}, the anodic peak current of Fc^+ at the ss-DNA/Au electrode increases obviously. The plot of anodic peak current ($i_{p,a}$) versus scan rate shows a linear relation with a relative coefficient (R) of 0.9957 (inset 1 in Fig.

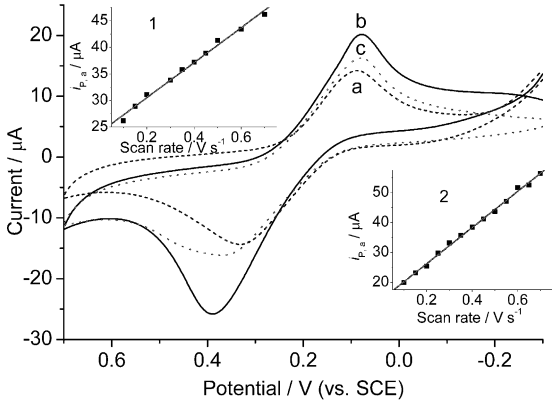

Fig. 1. Cyclic voltammograms of 8.0×10^{-4} mol l^{-1} $FcPF_6$ in 0.01 mol l^{-1} TE solution at TGA/Au (a), ss-DNA/Au (b) and ds-DNA/Au (c) electrodes at 100 mV s^{-1}. Insets: relationship between anodic peak current of $FcPF_6$ and scan rate at ss-DNA/Au (1) and ds-DNA/Au electrodes (2).

1). At the ds-DNA/Au electrode Fc^+ shows the same behavior (inset 2 in Fig. 1). Thus, the electrode reactions at both electrodes are a surface-controlled electrode process.

3.2. Effect of ion strength

In order to explore the interaction mechanism between Fc^+ and the immobilized ss- or ds-DNA, the same experiments were performed at the ss- and ds-DNA/Au electrodes by adding the different amount of NaCl (from 10^{-6} to 10^{-2} mol l^{-1}) to the $FcPF_6$ solution. Fig. 2 shows cyclic voltammograms of $FcPF_6$ in TE solution containing different concentrations of NaCl at the ss- or ds-DNA/Au electrodes. With increasing ion strength, the redox peak currents of $FcPF_6$ decrease, and the cathodic peak shifts to a more negative potential, indicative of a prevention to the reduction of Fc^+ and the interaction between Fc^+ and the immobilized ss- or ds-DNA due to the adsorption of Na^+. When NaCl concentration is up to 10^{-4} mol l^{-1}, no current peak can be detected over the cyclic voltammetric curves. Thus, the ion strength affects obviously the electrochemical behavior of Fc^+ at both ss- and the ds-DNA/Au electrodes. The interaction between Fc^+ and the ss- or ds-DNA/Au electrode is an electrostatic mechanism. The cationic Fc^+ molecules electrostatically associate with the anionic phosphate groups in DNA backbone. Furthermore, the electrostatic interaction between Fc^+ and the ds-DNA/Au electrode is weaker than that between Fc^+ and the ss-DNA helix, which results in a decrease in the redox peak currents or the amount of Fc^+ cation electrostatically bound to the anionic DNA backbone upon the hybridization procedure. This appearance is different from those reported previously by using a highly charged cation, such as Tris(2′2-bipyridyl)cobalt(III) or ruthenium hexaammine($^{3+/2+}$), as an electroactive indicator (Steel et al., 1998). This difference results from the different structures of the redox cations.

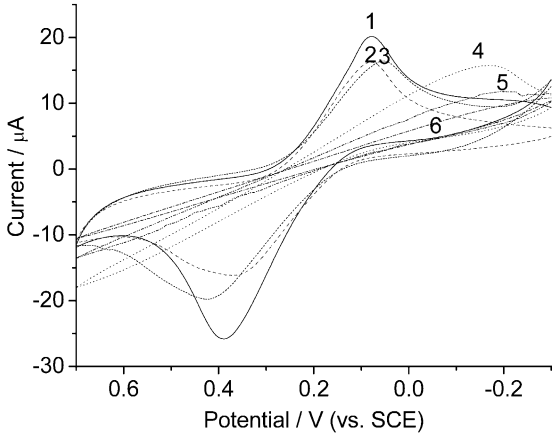

Fig. 2. Effect of ion strength on cyclic voltammogram of 8.0×10^{-4} mol l^{-1} $FcPF_6$ in 0.01 mol l^{-1} TE solution at ss-DNA/Au electrode at 100 mV s^{-1}. NaCl concentrations: 0 (1), 10^{-6} (2), 10^{-5} (3), 10^{-4} (4), 10^{-3} (5) and 10^{-2} mol l^{-1} (6).

The association constant between cations and DNA phosphate increases with the cation charge (Steel et al., 1998). The highly charged cation possesses much stronger binding ability than Fc^+ molecule. Thus, the effect of the amount of anionic phosphate group in DNA on the interaction between the highly charged cation and the buried phosphate group in ds-DNA helix is larger than that of the steric hindrance of ds-DNA backbone to the binding of cation, which results in an increase in the amount of redox cation electrostatically bound to the surface upon hybridization (Steel et al., 1998). On the other hand, the special steric structure of Fc^+ and the negatively charged ligands in Fc^+ molecule lead to a larger hindrance than other redox cations to bind to the buried phosphate group in ds-DNA helix. The burial of phosphate group in ds-DNA helix and the less negative charges on ds-DNA/Au surface are verified with the AC impedance experiments (shown in Section 3.3). Contrarily, lower steric hindrance of ss-DNA helix to the binding of Fc^+ molecules to phosphate group and more negative charges on ss-DNA/Au surface are favorable to the binding of Fc^+. Thus, a decrease in the amount of Fc^+ cation electrostatically bound to the surface upon hybridization is observed.

3.3. AC impedance spectra

The AC technique has been used in the study of electrochemical reaction. Its impedance experimental data are often plotted in a complex plane known as a Nyquist plot (as shown in Fig. 3). For a reversible electrode process the experimental curve displays a semicircle in high frequency range and a straight line with the slope of 1 in low frequency range. AC impedance measurements were performed at a given open circuit voltage with an amplitude of 5 mV and a frequency change over the range of 10^5–1 Hz. Fig. 3 shows the AC impedance spectra (Nyquist plot) of 8.0×10^{-4} mol l^{-1} $FcPF_6$ in 0.01 mol l^{-1} TE solution at bare gold (a), TGA/Au (b), ss-DNA/Au (c), and ds-DNA/Au (d) electrodes, respectively. From the plots, the values of R_s, and R_{ct} are obtained, as shown in Table 1. The R_s values obtained at the four electrodes are very close. But the value of R_{ct} at the ss-DNA/Au electrode is only half of those obtained at other electrodes. This result is different from that reported (Lee and Shim, 2001) due to the different detection mechanisms. The interaction between Fc^+ unit and DNA chain is an electrostatic mechanism. Thus, it is easier aggregated on immobilized ss-DNA surface due to the more naked negative-charged groups on the surface, resulting in a lower value of R_{ct} and a faster electron transfer rate. After hybridization of immobilized ss-DNA with

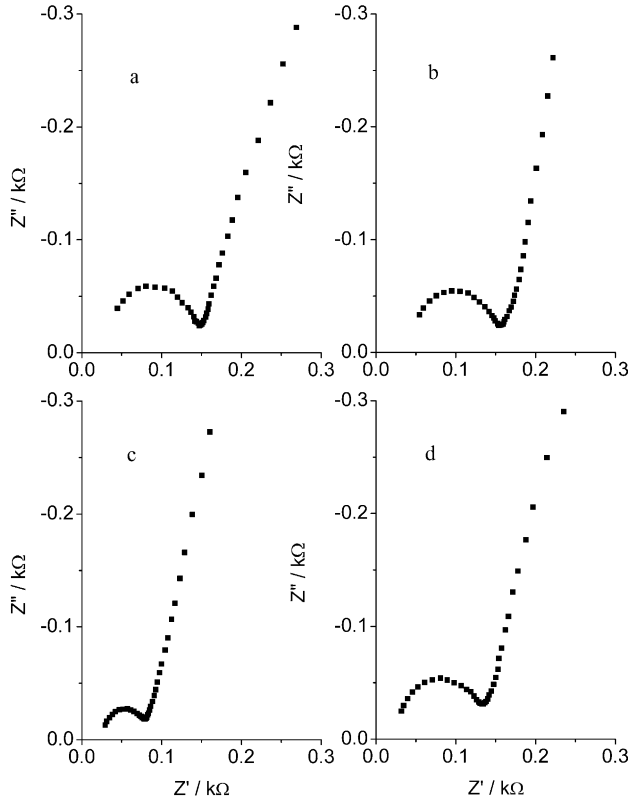

Fig. 3. AC impedance spectra of 8.0×10^{-4} mol l^{-1} $FcPF_6$ in 0.01 mol l^{-1} TE solution at bare (a), TGA/Au (b), ss-DNA/Au (c) and ds-DNA/Au (d) electrodes.

Table 1
AC impedance analysis of R_s, R_{ct} and C_d obtained from Nyquist plots

Parameters	Bare gold	TGA/Au	ss-DNA/Au	ds-DNA/Au
R_s (Ω)	44.7	48.9	28.7	31.9
R_{ct} (Ω)	102.4	109.3	51.9	101.7
C_d (μF cm^{-2})	0.59	0.55	1.39	0.87

cDNA, most of the negative charges on DNA chain are buried in ds-DNA helix, which makes the electrostatic interaction between Fc^+ and DNA surface weaker. Thus R_{ct} increases and the reaction rate decreases again. These results are consistent with the changes in peak currents of the cyclic voltammograms.

From the maximum value of Z'' at semicircle the characteristic angular frequency ω^* and double layer capacitance can be obtained. The C_d values of four systems are listed in Table 1. The C_d value at the TGA/Au electrode is slightly smaller than that at bare gold electrode, indicative of the presence of TGA monolayer on the electrode surface. The C_d value at the ss-DNA/Au electrode is obviously larger than other three systems because of more negative charges on the ss-DNA/Au surface, which possesses higher dielectric constant. The C_d value at the ds-DNA/Au electrode is larger than those at bare and the TGA/Au electrodes. The ds-DNA/Au electrode gives a smaller C_d value than the ss-DNA/Au electrode due to the burial of the negatively charged phosphate groups in ds-DNA helix.

3.4. XPS spectra

Fig. 4 shows the XPS spectra of the TGA/Au electrode (1) and the ss-DNA/Au electrode (2). The XPS spectra exhibit the peaks of C, O and S elements at the TGA/Au electrode and the peaks of C, O, S, N and P elements at the ss-DNA/Au electrode. The individual expanded spectra of P2p, S2p, C1s, N1s and O1s are given in Fig. 4b–f, respectively. The difference in peak intensity of S2p at the TGA/Au and ss-DNA/Au electrodes (Fig. 4c) results from their different structures. At the ss-DNA/Au electrode (curve 2) the peak of S2p is lower, which is attribute to the burying of S atom

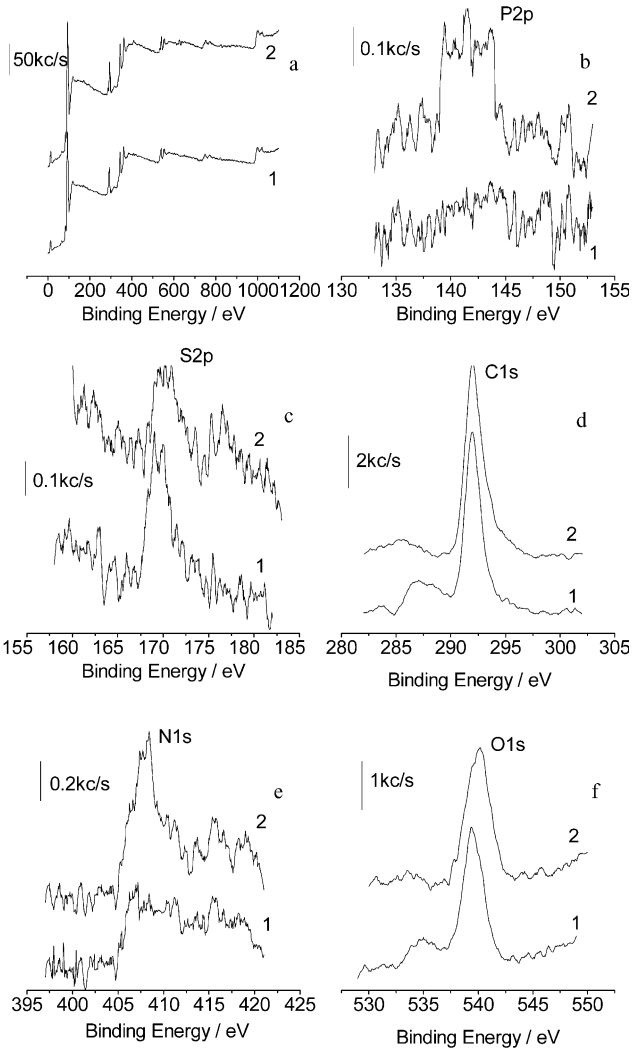

Fig. 4. XPS spectra of TGA/Au (1) and ss-DNA/Au (2) from 0 to 1200 eV (a), 130–150 eV for P2p spectrum (b), 155–185 eV for S2p spectrum (c), 280–305 eV for C1s spectrum (d), 395–415 eV for N1s spectrum (e) and 520–550 eV for O1s spectrum (f).

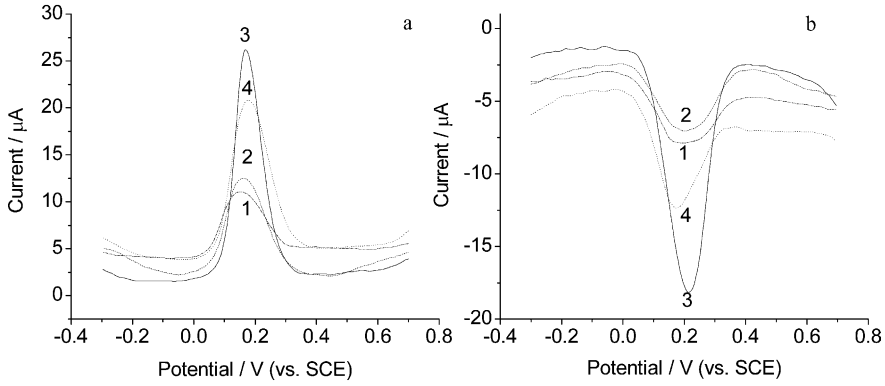

Fig. 5. Anodic (a) and cathodic (b) differential pulse voltammograms of 8.0×10^{-4} M $FcPF_6$ in 0.01 mol l^{-1} TE solution at bare (1), TGA/Au (2), ss-DNA/Au (3) and ds-DNA/Au (4) electrodes at 20 mV s^{-1}.

in DNA fragment. The peak of P2p shown in the curve 2 of Fig. 4b is the best evidence that ss-DNA has been covalently immobilized on the TGA self-assembled monolayer gold surface. The curve 2 of Fig. 4e shows a peak of N element, also indicative of the presence of ss-DNA on the electrode surface. From the peak areas of curve 2 in Fig. 4e and f, the molar ratio of N to O is calculated to be 1:1.82. It is known that the ratio of (G+C):(A+T) in this sequence-known HBV DNA fragment is 49:51. Thus, the value of N:O is calculated theoretically to be 1:1.87 in the HBV ss-DNA fragment. The experimental value of N:O obtained from XPS is near the theoretical value, verifying that the material immobilized on the gold electrode surface is HBV ss-DNA.

3.5. Differential pulse voltammetric experiments

The differential pulse voltammograms of 8.0×10^{-4} mol l^{-1} $FcPF_6$ at different electrodes were determined from -0.3 to $+0.7$ V (Fig. 5a) and $+0.7$ to -0.3 V (Fig. 5b) in 0.01 mol l^{-1} TE solution at 20 mV s^{-1}. The anodic peak currents of $FcPF_6$ at bare gold, TGA/Au, ss-DNA/Au and ds-DNA/Au electrodes were 3.86, 4.54, 16.18 and 6.60 μA, respectively, while the cathodic peak currents were 6.61, 7.45, 24.24 and 16.41 μA, respectively. The relative standard deviations of current detections for four times at the same electrodes were less than 3.0%. As obtained from the cyclic voltammograms, the redox peak currents of Fc^+ at the ss-DNA/Au electrode were the maximum due to the electrostatic adsorption of Fc^+ at ss-DNA/Au surface. The hybridization of the immobilized ss-DNA with cDNA resulted in a decrease of peak current. The anodic and cathodic peak currents decrease by 59.3 and 32.3%, respectively, due to the burial of the negatively charged groups in DNA chains during hybridization process, which resulted in less Fc^+ units were aggregated on immobilized ds-DNA surface with the electrostatic mechanism. As control, no observable change in peak currents of the differential pulse voltammograms of $FcPF_6$ was observed after the covalently immobilized HBV ss-DNA was treated with the same process in the solution containing denatured calf-thymus ss-DNA or yeast DNA samples, indicating that they did not hybridize with the immobilized HBV ss-DNA. Thus, both cyclic voltammetric and differential pulse voltammetric techniques could be used for recognition of HBV ss-DNA immobilized on electrode surface to its cDNA with Fc^+ as an electroactive indicator.

4. Conclusions

An electrochemical hybridization biosensor has been prepared for detection of short-stranded HBV DNA. The immobilization of ss-DNA on Au surface is verified by AC impedance and XPS spectra. The interaction between $FcPF_6$ and HBV ss- or ds-DNA immobilized on electrode surface shows an electrostatic mechanism. Using cyclic voltammetric and differential pulse voltammetric techniques, the DNA biosensor has successfully been used for the hybridization recognition with a high selectivity. This method provides a highly sensitive detection of DNA of 1×10^4 copies (about 1.7×10^{-20} mol) of original genomic HBV DNA by combining a PCR procedure.

Acknowledgements

This work was supported by the National Natural Science Foundation of China (20275017, 29835110 and 29975013), the Science Foundation of Jiangsu (BS2001063), the Specialized Research Fund for the Doctoral Program of Higher Education from Ministry of Education of China (200028403) and State Key Laboratory of Electroanalytical Chemistry, Changchun Institute of Applied Chemistry.

References

Beasley, R.P., 1988. Hepatitis B virus—the major etiology of hepatocellular carcinoma. Cancer 61, 1942–1956.

Bianchi, N., Rutigliano, C., Tomassetti, M., Feriotto, G., Zorzato, F., Gambari, R., 1997. Biosensor technology and surface plasmon resonance for real-time detection of HIV-1 genomic sequences amplified by polymerase chain reaction. Clin. Diagn. Virol. 8, 199–208.

Buffello-Le Guillou, D., Duclos-Vallee, J.C., Eberle, F., Capel, F., Petit, M.A., 2000. Evaluation of an enzyme-linked immunosorbent assay for detection and quantification of hepatitis B virus PreS1 envelope antigen in serum samples: comparison with two commercial assays for monitoring hepatitis B virus DNA. J. Viral Hepatitis 7, 387–392.

Carter, M.T., Rodriguez, M., Bard, A.J., 1989. Voltammetric studies of the interaction of metal chelates with DNA. 2. Tris-chelated complexes of cobalt(III) and iron(II) with 1,10-phenanthroline and 2,2′-bipyridine. J. Am. Chem. Soc. 111, 8901–8911.

Chemin, I., Zoulim, F., Merle, P., Arkhis, A., Chevallier, M., Kay, A., Cova, L., Chevallier, P., Mandrand, B., Trepo, C., 2001. High incidence of hepatitis B infections among chronic hepatitis cases of unknown aetiology. J. Hepatol. 34, 447–454.

Chen, X., Zhang, X.E., Chai, Y.Q., Hu, W.P., Zhang, Z.P., Zhang, X.M., Cass, A.E.G., 1998. DNA optical sensor: a rapid method for the detection of DNA hybridization. Biosens. Bioelectron. 13, 451–458.

Chen, R.W., Piiparinen, H., Seppanen, M., Koskela, P., Sarna, S., Lappalainen, M., 2001. Real-time PCR for detection and quantitation of hepatitis B virus DNA. J. Med. Virol. 65, 250–256.

Erdem, A., Kerman, K., Meric, B., Akarca, U.S., Ozsoz, M., 2000. Novel hybridization indicator methylene blue for the electrochemical detection of short DNA sequences related to the hepatitis B virus. Anal. Chim. Acta 422, 139–149.

Gilbert, N., Corden, S., Ijaz, S., Grant, P.R., Tedder, R.S., Boxall, E.H., 2002. Comparison of commercial assays for the quantification of HBV DNA load in health care workers: calibration differences. J. Virol. Methods 100, 37–47.

Hashimoto, K., Ito, K., Ishimori, Y., 1998. Microfabricated disposable DNA sensor for detection of hepatitis B virus DNA. Sens. Actuat. B-Chem. 46, 220–225.

He, F.J., Zhang, L.D., 2002. Rapid diagnosis of M-tuberculosis using a piezoelectric immunosensor. Anal. Sci. 18, 397–401.

Heijtink, R.A., Janssen, H.L.A., Hop, W.C.J., Osterhaus, A.D.M.E., Schalm, S.W., 2001. Interferon-alpha therapy for chronic hepatitis B: early response related to pre-treatment changes in viral replication. J. Med. Virol. 63, 217–219.

Hwang, S.J., Lu, R.H., Wood, M.L., Wang, Y.J., Chang, F.Y., Lee, S.D., 1999. Comparison of the nucleic acid-based crosslinking hybridization assay and the branched DNA signal amplification assay in the quantitative measurement of serum hepatitis B virus DNA. J. Clin. Lab. Anal. 13, 296–300.

Jiang, X.P., Xu, D.K., Liu, Y.Q., Ma, L.R., 2000. Chemiluminescencent biosensor for nucleic acid. Chin. J. Anal. Chem. 28, 12–16.

Kimura, T., Rokuhara, A., Sakamoto, Y., Yagi, S., Tanaka, E., Kiyosawa, K., Maki, N., 2002. Sensitive enzyme immunoassay for hepatitis B virus core-related antigens and their correlation to virus load. J. Clin. Microbiol. 40, 439–445.

Krajden, M., 1999. Hepatitis B virus: detection and quantitation by membrane and liquid hybridization, branched DNA signal amplification, hybrid capture, and PCR methods. Methods Mol. Med. 20, 103–128.

Lai, V.C.H., Guan, R., Wood, M.L., Lo, S.K., Yuen, M.F., Lai, C.L., 1999. Nucleic acid-based cross-linking assay for detection and quantification of hepatitis B virus DNA. J. Clin. Microbiol. 37, 161–164.

Lee, T.Y., Shim, Y.B., 2001. Direct DNA hybridization detection based on the oligonucleotide-functionalized conductive polymer. Anal. Chem. 73, 5629–5632.

Loeb, K.R., Jerome, K.R., Goddard, J., Huang, M.L., Cent, A., Corey, L., 2000. High-throughput quantitative analysis of hepatitis B virus DNA in serum using the TaqMan fluorogenic detection system. Hepatology 32, 626–629.

Marrazza, G., Chianella, I., Mascini, M., 1999. Disposable DNA electrochemical biosensors for environmental monitoring. Anal. Chim. Acta 387, 297–307.

Marrazza, G., Chiti, G., Mascini, M., Anichini, M., 2000. Detection of human apolipoprotein E genotypes by DNA electrochemical biosensor coupled with PCR. Clin. Chem. 46, 31–37.

Mei, S.D., Yatsuhashi, H., Parquet, M.D., Hamada, R., Fujino, T., Matsumoto, T., Inoue, O., Koga, M., Yano, M., 2000. Detection of HBV RNA in peripheral blood mononuclear cells in patients with and without HBsAg by reverse transcription polymerase chain reaction. Hepatol. Res. 18, 19–28.

Mendy, M.E., Fortuin, M., Hall, A.J., Jack, A.D., Whittle, H.C., 1999. Hepatitis B virus DNA in relation to duration of hepatitis B surface antigen carriage. Br. J. Biomed. Sci. 56, 34–38.

Mercier, B., Burlot, L., Ferec, C., 1999. Simultaneous screening for HBV DNA and HCV RNA genomes in blood donations using a novel TaqMan PCR assay. J. Virol. Methods 77, 1–9.

Meric, B., Kerman, K., Ozkan, D., Kara, P., Erensoy, S., Akarca, U.S., Mascini, M., Ozsoz, M., 2002. Electrochemical DNA biosensor for the detection of TT and hepatitis B virus from PCR amplified real samples by using methylene blue. Talanta 56, 837–846.

Ngui, S.L., Hallet, R., Teo, C.G., 1999. Natural and iatrogenic variation in hepatitis B virus. Rev. Med. Virol. 9, 183–209.

Paleček, E., Fojta, M., 2001. Detecting DNA hybridization and damage. Anal. Chem. 73, 74A–83A.

Pas, S.D., Fries, E., De Man, R.A., Osterhaus, A.D.M.E., Niesters, H.G.M., 2000. Development of a quantitative real-time detection assay for hepatitis B virus DNA and comparison with two commercial assays. J. Clin. Microbiol. 38, 2897–2901.

Pawlotsky, J.M., Bastie, A., Lonjon, I., Remire, J., Darthuy, F., Soussy, C.J., Dhumeaux, D., 1997. What technique should be used for routine detection and quantification of HBV DNA in clinical samples. J. Virol. Methods 65, 245–253.

Poljak, M., Marin, I.J., Seme, K., Brinovec, V., Maticic, M., Meglic-Volkar, J., Lesnicar, G., Vince, A., 2001. Second-generation hybrid capture test and amplicor monitor test generate highly correlated hepatitis B virus DNA levels. J. Virol. Methods 97, 165–169.

Rodriguez, M., Bard, A.J., 1990. Electrochemical studies of the interaction of metal chelates with DNA. 4. Voltammetric and electrogenerated chemiluminescent studies of the interaction of tris(2,2′-bipyridine) osmium(II) with DNA. Anal. Chem. 62, 2658–2662.

Rogers, K.R., Apostol, A., Madsen, S.J., Spencer, C.W., 2001. Fiber optic biosensor for detection of DNA damage. Anal. Chim. Acta 444, 51–60.

Sato, S., Ohhashi, W., Ihara, H., Sakaya, S., Kato, T., Ikeda, H., 2001. Comparison of the sensitivity of NAT using pooled donor samples for HBV and that of a serologic HBsAg assay. Transfusion 41, 1107–1113.

Shintani, Y., Yotsuyanagi, H., Moriya, Y., Fujie, H., Tsutsumi, T., Takayama, T., Makuuchi, M., Kimura, S., Koike, K., 2000. The significance of hepatitis B virus DNA detected in hepatocellular carcinoma of patients with hepatitis C. Cancer 88, 2478–2486.

Steel, A.B., Heme, T.M., Tarlov, M.J., 1998. Electrochemical quantitation of DNA immobilized on gold. Anal. Chem. 70, 4670–4677.

Wang, J., 1999. Electroanalysis and biosensors. Anal. Chem. 71, 328–332.

Wang, J., Rivas, G., Cai, X.H., Chicharro, M., Parrado, C., Dontha, N., Begleiter, A., Mowat, M., Palecek, E., Nielsen, P.E., 1997.

Detection of point mutation in the p53 gene using a peptide nucleic acid biosensor. Anal. Chim. Acta 344, 111–118.

Weber, B., Melchior, W., Gehrke, R., Doerr, H.W., Berger, A., Rabenau, H., 2001. Hepatitis B virus markers in anti-HBc only positive individuals. J. Med. Virol. 64, 312–319.

Yates, S., Penning, M., Goudsmit, J., Frantzen, I., van de Weijer, B., van Strijp, D., van Gemen, B., 2001. Quantitative detection of hepatitis B virus DNA by real-time nucleic acid sequence-based amplification with molecular beacon detection. J. Clin. Microbiol. 39, 3656–3665.

Yoshiko, N., 1999. The role of genetic diagnosis in clinics. From the choice of ordering until reading the data. Rinsho Byori 47, 1006–1013.

Zhao, Y.D., Pang, D.W., Wang, Z.L., Cheng, J.K., Qi, Y.P., 1997. DNA-modified electrodes 2. Electrochemical characterization of gold electrodes modified with DNA. J. Electroanal. Chem. 431, 203–209.

Zhao, Y.D., Pang, D.W., Hu, S., Wang, Z.L., Cheng, J.K., Dai, H.P., 1999. DNA-modified electrodes, part 4: optimization of covalent immobilization of DNA on self-assembled monolayers. Talanta 49, 751–756.